ZEOLITE CATALYSIS

Role of the ionic environment in enhancing the activity of reacting molecules in zeolite pores

Niklas Pfriem[1], Peter H. Hintermeier[1], Sebastian Eckstein[1], Sungmin Kim[2], Qiang Liu[1,3], Hui Shi[1,4], Lara Milakovic[1], Yuanshuai Liu[1,5], Gary L. Haller[1], Eszter Baráth[1], Yue Liu[1]*, Johannes A. Lercher[1,2]*

Tailoring the molecular environment around catalytically active sites allows for the enhancement of catalytic reactivity through a hitherto unexplored pathway. In zeolites, the presence of water creates an ionic environment via the formation of hydrated hydronium ions and the negatively charged framework aluminum tetrahedra. The high density of cation-anion pairs determined by the aluminum concentration of a zeolite induces a high local ionic strength that increases the excess chemical potential of sorbed and uncharged organic reactants. Charged transition states (carbocations for example) are stabilized, which reduces the energy barrier and leads to higher reaction rates. Using the intramolecular dehydration of cyclohexanol on H-MFI zeolites in water, we quantitatively show an enhancement of the reaction rate by the presence of high ionic strength as well as show potential limitations of this strategy.

Zeolites, which are Brønsted- or Lewis-acidic microporous tectosilicates, are widely applied in chemical industry for sorption, separation, and catalysis (*1*–*4*). In the most classic case, the acid character is introduced by substitution of metal cations with a 3+ formal charge (*5*). It has been speculated that the proximity of charge and dipoles in zeolite pores should give rise to strong field effects, but the effects were not systematically quantifiable (*6*, *7*). A long series of investigations has shown that Brønsted acid sites (BASs) have constant acid strength for sorption and catalysis, as long as the concentrations of substituting tetrahedral atoms do not exceed a certain threshold (*8*, *9*). The high intrinsic catalytic activity of zeolites has, therefore, been attributed to the notable stabilization of transition states in the constraints of pores (*10*–*14*).

Recent experiments have shown that this beneficial aspect of transition-state stabilization also holds true when the catalyzed reaction is performed in the presence of water, allowing for the generation of hydrated hydronium ions ($H_3O^+_{hydr.}$). The catalytic activity of these hydronium ions is up to two orders of magnitude higher than the respective specific activity of $H_3O^+_{hydr.}$ in an aqueous acid solution, as probed by alcohol dehydration (*10*, *11*, *15*). In the environment of the zeolites, the $H_3O^+_{hydr.}$ occupy a well-defined location at aluminum tetrahedra (which causes the BAS in the solid) and are located in much closer proximity in zeolite pores than in the liquid phase. This proximity has been shown to lead to an increase in the activity coefficient of organic molecules in the zeolite pores, resembling the situation in the aqueous phase in the presence of high concentrations of cations and anions of dissolved acids, bases, and salts (*15*). The direct consequence of the higher activity coefficient is a decrease in the interaction strength of the sorbed organic molecules, much like the decreasing interaction with the solvent in an aqueous solution of increasing density of cation-anion pairs. This allows for a rigorous translation of the physical chemistry of nonideality in an aqueous phase into the constraints of nanopores.

The higher activity coefficient is caused by an increase in the excess chemical potential compared with an ideal environment, for example, of a zeolite having no BAS. Conceptually, the increase in the excess chemical potential of the reacting molecule decreases the energy difference to the transition state and, in consequence, should lead to a higher rate, even if the transition state is not stabilized. In addition, a polar transition state will be stabilized by the polar environment compared with the uncharged reactant. The confinement and the well-defined close spacing of $H_3O^+_{hydr.}$ additionally stabilize the transition state, acting positively to reduce the free-energy barrier in the confines of zeolites (*10*, *11*).

Here, we show that such a scenario can be realized and that the combination of the increase in the thermodynamic activity of reacting molecules and the steric constraints of the zeolite pores leads to strong deviations from the expected sympathetic variation of catalytic activities with active sites of constant acid-base properties. We use the dehydration of cyclohexanol on a series of H-MFI zeolites with a wide range of BAS [$H_3O^+_{hydr.}$] [0.05 to 0.86 millimoles per gram of MFI (mmol/g_{MFI})] to show that the positive effect of enhancing the excess chemical potential of reacting molecules leads to an optimum density of active sites.

When catalyzed by $H_3O^+_{hydr.}$, cyclohexanol dehydrates to cyclohexene in the aqueous phase on zeolite H-MFI. The reaction rate is independent of the aqueous phase concentration of cyclohexanol above 0.1 mol/liter (zero-order-reaction region; fig. S1). The rate normalized to the concentration of BAS, the turnover frequency (TOF), increased sixfold from a BAS concentration of 0.054 to 0.36 mmol/g_{MFI} and then decreased by 60% to a BAS concentration of 0.86 mmol/g_{MFI} (Fig. 1A). Concurrently, the activation energy decreased from 161 to 140 kJ/mol and increased to 158 kJ/mol afterward (Fig. 1B). By contrast, for gas phase reactions such as *n*-pentane cracking and 1-propanol dehydration, the variation in BAS concentration did not change the TOF, that is, the acid strength of the sites involved can be considered as being constant (Fig. 1C). The identical catalytic activity of BASs in such a series of zeolites has been shown before for cracking (*16*, *17*). The characterization with a base molecule also showed an identical strength of the BAS (*18*). Although it has been reported that different Al locations influence the catalytic activity of zeolites (*19*, *20*), the constant TOFs of *n*-pentane cracking and 1-propanol dehydration on all the tested H-MFIs allow us to exclude the probability that selective Al locations on any specific T sites or in pairs affect reactivity.

Then, the question arises as to why BASs exhibited substantial differences in the presence of water. To address this question, we analyzed the differences of BASs induced by their environments. In the gas phase, BASs are predominately covalent hydroxy groups, located on oxygen bridging between silicon-oxygen and aluminum-oxygen tetrahedra in the zeolite. The hydroxy groups are moderately polar and have negligible volume. In water, the BASs are converted to $H_3O^+_{hydr.}$ bonded ionically to the zeolite framework, with a positive charge and a specific volume.

In contrast to a homogeneous solution in which $H_3O^+_{hydr.}$ are highly dispersed throughout the liquid volume, the $H_3O^+_{hydr.}$ in H-MFI are confined in the limited space of zeolite pores. Consequently, this leads to a very high local concentration that cannot be changed by adding more water. Figure 2A (black line) shows the concentrations of $H_3O^+_{hydr.}$ per H-MFI unit cell varying between 0.3 and 5 in the samples tested, corresponding to a local density of 0.1 to 1.6 mol/liter, using the H-MFI unit cell volume of about 5.2 nm^3 (*21*). If we

[1]Department of Chemistry and Catalysis Research Center, Technical University of Munich, Lichtenbergstrasse 4, 85747 Garching, Germany. [2]Institute for Integrated Catalysis, Pacific Northwest National Laboratory, P.O. Box 999, Richland, WA 99352, USA. [3]Paul Scherrer Institute, Forschungsstrasse 111, 5232 Villigen PSI, Switzerland. [4]School of Chemistry and Chemical Engineering, Yangzhou University, Siwangting Road 180, 225009 Yangzhou, Jiangsu, China. [5]Qingdao Institute of Bioenergy and Bioprocess Technology, Chinese Academy of Sciences, Songling Road 189, Laoshan District, Qingdao, China.
*Corresponding author. Email: yue.liu@tum.de (Y.L.); johannes.lercher@tum.de (J.A.L.)

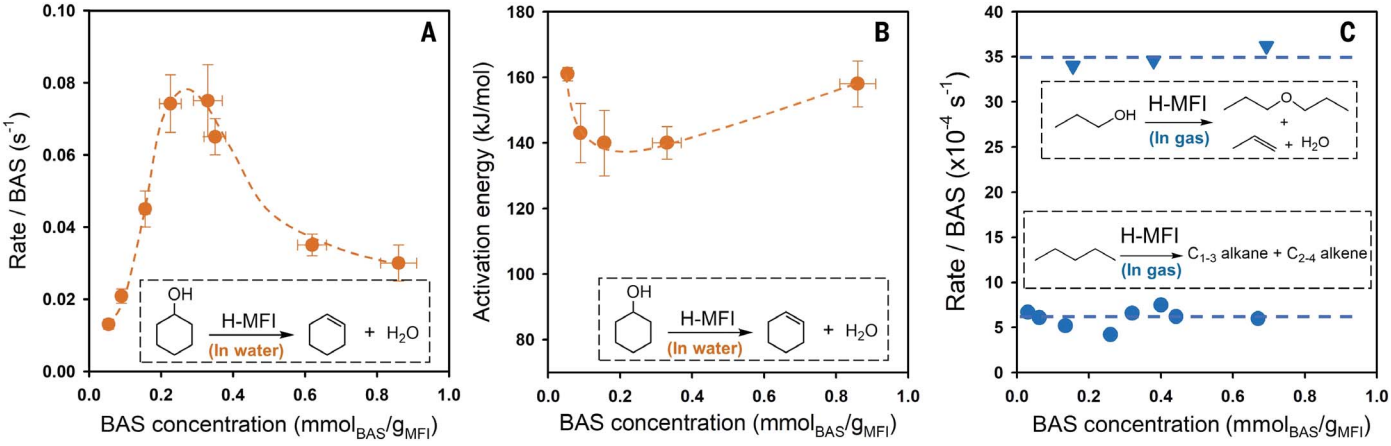

Fig. 1. BAS-normalized reaction rate in H-MFI–catalyzed reactions in water and gas phases. (**A** and **B**) Rate at 423 K (A) and activation energy (B) of cyclohexanol dehydration on H-MFI with different BAS concentrations in water. (**C**) Cracking of *n*-pentane at 763 K (circles) and dehydration of 1-propanol at 433 K (triangles) on H-MFI with different BAS concentrations in the gas phase. Data for *n*-pentane cracking are from (*25*) and (*16*); data for 1-propanol dehydration on H-MFI with 0.69 mmol/g_{MFI} are from (*26*).

consider further that the micropore volume of H-MFI is only ~1.3 nm^3 per unit cell (~0.14 cm^3/g_{MFI}; table S1), then the $H_3O^+_{hydr.}$ has a molarity in the range of 0.4 to 6.4 mol/liter in the micropore space. Such high local concentrations of $H_3O^+_{hydr.}$ have two consequences: a very high local ionic strength and a competition between the $H_3O^+_{hydr.}$ and the substrate for the micropore space.

As an ion pair, $H_3O^+_{hydr.}$ with the corresponding anions induces an ionic environment. In an aqueous homogeneous electrolyte solution, this leads to nonideality by which the ions (including $H_3O^+_{hydr.}$) have concentration-dependent activity coefficients (γ). A solute is stabilized ($\gamma < 1$) or destabilized ($\gamma > 1$) by the presence of a specific concentration of cations and anions, reflecting an increased or decreased excess chemical potential of the solute. The ionic strength (I) is the most critical variable determining the extent of deviation from an ideal solution. It is defined as the sum of the product of the charge (z_i) squared and the concentration (c_i) of all the ions (Eq. 1). Thus, γ is expressed as a function of I, $\gamma(I)$:

$$I = \frac{1}{2} \cdot \sum c_i z_i^2 \qquad (1)$$

Although classical ionic strength is defined for a homogeneous solution, we have shown previously that the concept of nonideality and ionic strength is transferrable to zeolites in water and applicable to quantitatively explain adsorption properties (*15*). By considering the zeolite to be a "quasi solid electrolyte," its local ionic strength in a micropore is also defined by Eq. 1, with z_i being 1 and c_i being volumetric densities of $H_3O^+_{hydr.}$ and the negatively charged framework site (Z^-) in the micropores, i.e., concentration normalized to micropore volume. Figure 2A (blue line) shows the ionic strength of the investigated H-MFI. The high local concentration of $H_3O^+_{hydr.}$ in H-MFI micropores induces high local ionic strength. For example, H-MFI (Si/Al 15) has a BAS concentration of 0.86 ± 0.05 mol/g_{MFI}, corresponding to an ionic strength of 4.9 ± 0.3 mol/liter. The ionic strength increases monotonically with the BAS concentration (Fig. 2A), and the curve bends at high BAS concentration, because of the expansion of the unit cell at high Al concentration that dilutes the volumetric concentration of $H_3O^+_{hydr.}$.

The nonideality also affects the catalytic reaction rate. In general, the TOF under a certain ionic strength TOF(I) differs from that under ideal conditions $TOF_{(ideal)}$—that is, TOF at zero ionic strength—by factors of the activity coefficient of ground state $\gamma_{GS}(I)$ and transition state $\gamma_{TS}(I)$ (Eq. 2A; detailed derivations are in supplementary text S1 and S2). The $TOF_{(ideal)}$ is determined by $\Delta G^{o\ddagger}_{(ideal)}$, which is the free-energy barrier under the ideal condition calculated by applying the transition-state formula (Eq. 2B):

$$TOF(I) = TOF_{(ideal)} \cdot \frac{\gamma_{GS}(I)}{\gamma_{TS}(I)} \qquad (2A)$$

$$TOF_{(ideal)} = \frac{k_B T}{h} \exp\left(-\frac{\Delta G^{o\ddagger}_{(ideal)}}{RT}\right) \qquad (2B)$$

where k_B, T, h, and R denote the Boltzmann constant, temperature, Plank constant, and ideal gas constant, respectively. The activity coefficient determines the excess chemical potential (μ^{excess}) according to $\mu^{excess} = RT\ln\gamma$. For the dehydration of cyclohexanol by $H_3O^+_{hydr.}$, it proceeds stepwise via association with $H_3O^+_{hydr.}$, protonation of the OH group, C–O cleavage to form the cyclohexyl carbenium ion, and deprotonation of the cyclohexyl carbenium ion (Fig. 2B). This stepwise mechanism is shown to dominate from low $H_3O^+_{hydr.}$ concentration (<0.01 mol/liter) in homogeneous acids to high local $H_3O^+_{hydr.}$ concentration (~2.7 mol/liter) in zeolites (*10*, *11*). The free-energy barrier is the energy difference between the transition state, the deprotonation of cyclohexyl carbenium ion by water ($C_6H_{11}^+\cdots H_2O$), and the ground state of adsorbed cyclohexanol associated with $H_3O^+_{hydr.}$ ($H_3O^+_{hydr.}\cdots C_6H_{11}OH$). Cyclohexanol is a neutral molecule in the ground state, whereas it is a positively charged cyclohexyl carbenium ion ($C_6H_{11}^+$) in the transition state. A neutral molecule is normally destabilized by the specific ionic strength ($\mu^{excess}_{GS} > 0$), given by Eq. 3A, which shows a proportional increase with I. The term K_s denotes the Setschenow constant. By contrast, a cation or an anion is normally stabilized by the presence of an ionic environment ($\mu^{excess}_{TS} < 0$), given by the extended Debye-Hückel equation (e.g., Truesdell-Jones equation; Eq. 3B), where a is the ion diameter and A, B, and b are constants:

$$\mu^{excess}_{GS} = 2.303 \cdot RTK_s I \qquad (3A)$$

$$\mu^{excess}_{TS} = 2.303RT \cdot \left(-\frac{A\sqrt{I}}{1 + aB\sqrt{I}} + bI\right) \qquad (3B)$$

As illustrated in Fig. 2B, the positive μ^{excess}_{GS} and negative μ^{excess}_{TS} in an ionic environment lead to a lower energy barrier compared with that under ideal conditions [$\Delta G^{o\ddagger}(I) < \Delta G^{o\ddagger}_{(ideal)}$].

The rate of cyclohexanol dehydration by HCl in homogeneous aqueous solution showed a

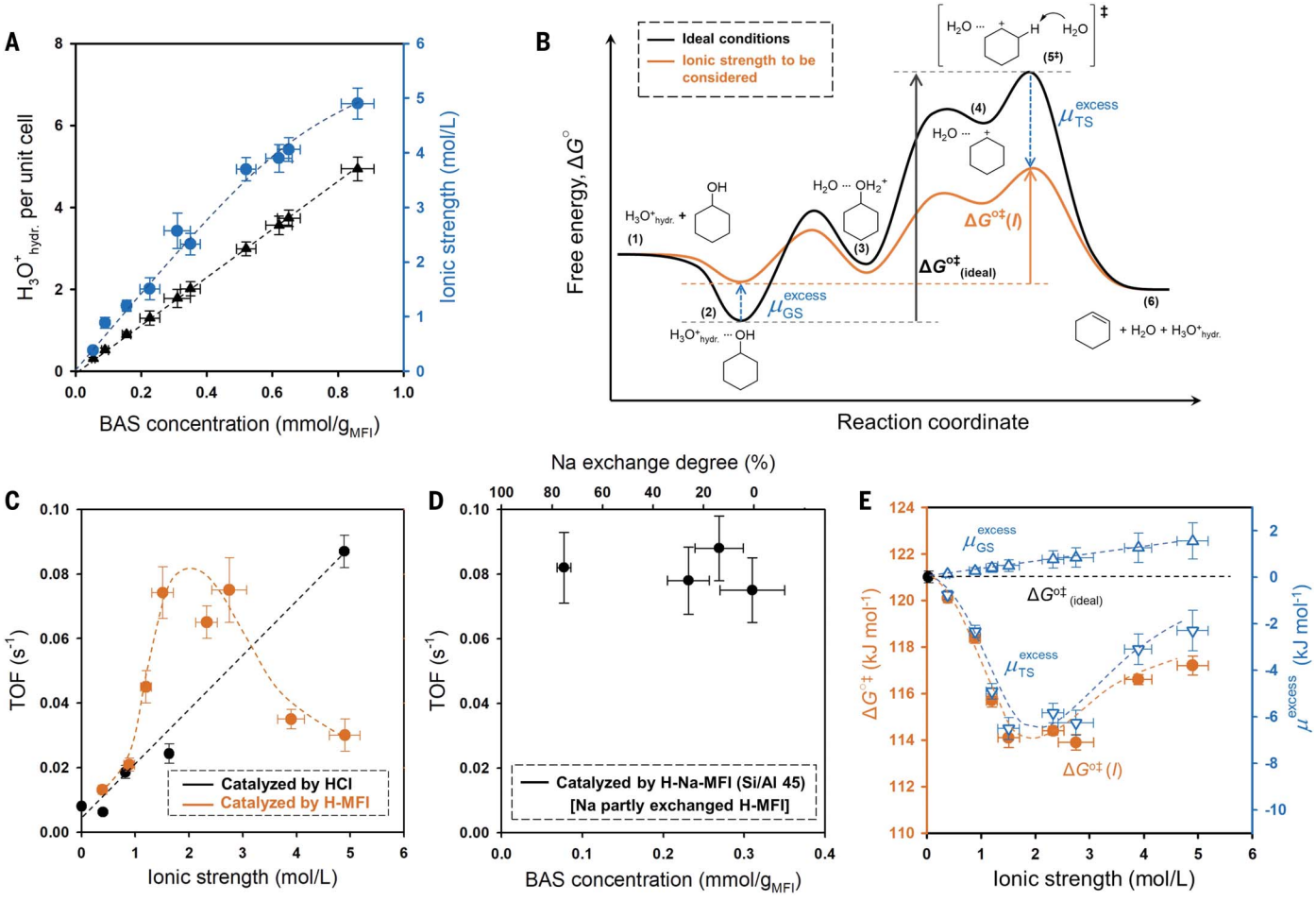

Fig. 2. Impact of local $H_3O^+_{hydr.}$ concentration and ionic strength on the dehydration of cyclohexanol catalyzed by $H_3O^+_{hydr.}$. (**A**) Unit cell–normalized concentrations of $H_3O^+_{hydr.}$ (triangles) and ionic strength (circles) as a function of BAS ($H_3O^+_{hydr.}$) concentration. (**B**) Elementary steps and their energies in dehydration of cyclohexanol on $H_3O^+_{hydr.}$ in H-MFI zeolite in water under ideal and nonideal conditions: (1) reactant cyclohexanol and $H_3O^+_{hydr.}$, (2) cyclohexanol associated with $H_3O^+_{hydr.}$, (3) protonated cyclohexanol, (4) cyclohexyl carbenium ion, ($5^‡$) transition state of deprotonation of cyclohexyl carbenium ion by water, and (6) product cyclohexene, water, and $H_3O^+_{hydr.}$. The "H_2O⋯" represents the interactions with solvent water. (**C**) TOF as a function of ionic strength under the catalysis of HCl (black circles) at 453 K and H-MFI (orange circles) at 423 K. The ionic strength in HCl solution is varied by changing the concentration of LiCl electrolyte. (**D**) TOF of Na partly exchanged H-MFI (Si/Al 45). (**E**) Reaction free-energy barriers and excess chemical potential of the ground state (GS) and transition state (TS) under the ideal condition and under an ionic strength. The calculations of free-energy barriers and excess chemical potential are provided in supplementary text S1.

positive correlation with the ionic strength in concentrated LiCl solution (black line in Fig. 2C). Its TOF at 453 K is less than 0.01 s^{-1} at very low ionic strength, whereas it increased to more than 0.08 s^{-1} at a high ionic strength of ~5 mol/liter. In analogy to HCl, the TOF of cyclohexanol dehydration on H-MFI is replotted as a function of ionic strength (orange line in Fig. 2C). It increases with increasing ionic strength up to ~2 mol/liter; however, in contrast to HCl, it drops at higher ionic strength.

To further explore the impact of ionic strength, a series of Na^+ partly exchanged H-MFI (Si/Al 45) were prepared. Partly exchanging $H_3O^+_{hydr.}$ by Na^+ decreases the BAS concentration of H-MFI while maintaining the same ionic strength. As shown in Fig. 2D, with Na exchange degrees up to 75%, the TOFs of H-Na-MFI remained unchanged, indicating that the variation of the concentration of $H_3O^+_{hydr.}$ while maintaining a constant ionic strength does not change the reaction rate. The comparison of H-Na-MFI (Si/Al 45) with a Na^+ exchange degree of 75% with H-MFI (Si/Al 200) exemplifies the impact of the ionic strength. Both samples have close BAS concentrations (77 versus 90 μmol/g_{MFI}); however, the former has a higher ionic strength than the latter (2.6 versus 0.9 mol/liter), and, indeed, the TOF is fourfold higher on H-Na-MFI (Si/Al 45) than on H-MFI (Si/Al 200), that is, 0.082 versus 0.021 s^{-1}. Thus, these results demonstrate that it is not the location of hydronium ions or the hydronium ion concentrations but the ionic strength that is critical for the specific catalyzed rate.

The free-energy barrier and excess chemical potential in the reactions are shown in Fig. 2E. The decrease of μ^{excess}_{TS} is more important than the increase of μ^{excess}_{GS}; thus, the lower free-energy barrier is mostly caused by the stabilization of the transition state. The inverse-volcano trend of μ^{excess}_{TS} with ionic strength seems at first sight consistent with Eq. 3B whereby the negative first term dominates at low ionic strength and the positive second term dominates at high ionic strength. However, the monotonic increase of TOFs with ionic strength at all concentrations under HCl catalysis excludes this possibility.

Next, we explore the reason for the rate drop with $H_3O^+_{hydr.}$ at higher concentrations. In contrast to catalysis in aqueous HCl, in H-MFI, both cyclohexanol and $H_3O^+_{hydr.}$ reside in the

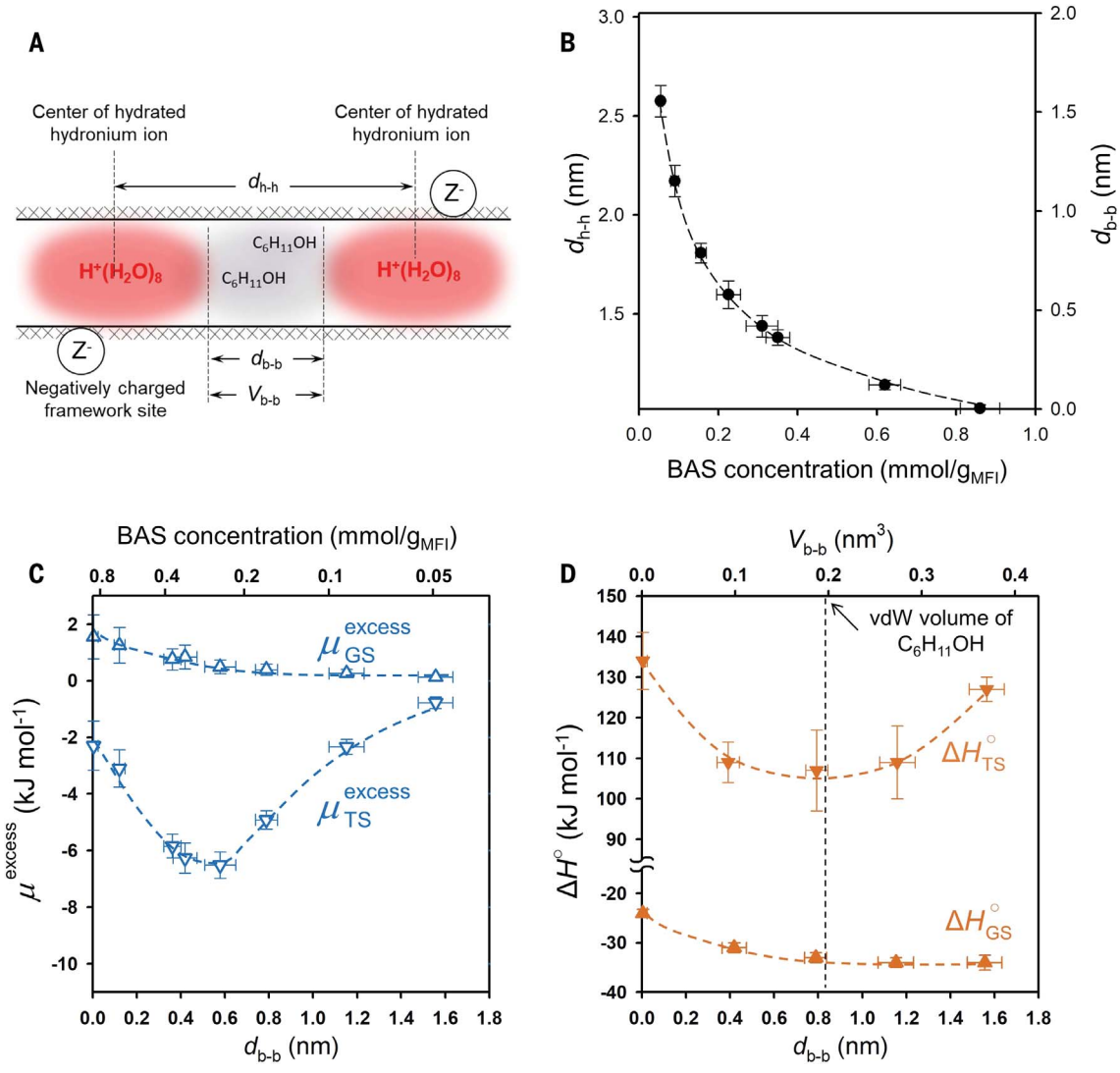

Fig. 3. Impact of the distance between $H_3O^+_{hydr.}$ in the H-MFI micropore on the energy of the ground state and the transition state of cyclohexanol dehydration catalyzed by $H_3O^+_{hydr.}$. (**A**) Schematic illustration of $H_3O^+_{hydr.}$ and cyclohexanol in H-MFI micropore channels and the mean distance $d_{h\text{-}h}$ between two neighboring $H_3O^+_{hydr.}$ and the mean distance $d_{b\text{-}b}$ and volume $V_{b\text{-}b}$ between the boundaries of neighboring $H_3O^+_{hydr.}$. (**B**) The $d_{h\text{-}h}$ and $d_{b\text{-}b}$ as a function of BAS concentration. (**C** and **D**) Excess chemical potential (C) and enthalpy of the ground and transition states (D) as a function of $d_{b\text{-}b}$ and $V_{b\text{-}b}$. The $d_{h\text{-}h}$ is estimated by the cubic root of the average zeolite volume normalized to the number of $H_3O^+_{hydr.}$; the $d_{b\text{-}b}$ is calculated by subtracting the length of $H_3O^+_{hydr.}$ from $d_{h\text{-}h}$; the $V_{b\text{-}b}$ is calculated by a cylinder model with length of $d_{b\text{-}b}$ and the diameter of the H-MFI micropore channel.

zeolitic micropore channels, and their relative locations are depicted in Fig. 3A. The average distance between two $H_3O^+_{hydr.}$ neighbors ($d_{h\text{-}h}$) represents the distance between $H_3O^+_{hydr.}$-Z^- pairs. The distance between their boundaries is $d_{b\text{-}b}$, with a volume of $V_{b\text{-}b}$. In the space between them resides the sorbed cyclohexanol. At the molecular level, the change of electrolyte concentration is equivalent to the change of $d_{h\text{-}h}$ and $d_{b\text{-}b}$. Thus, the increase of BAS concentration in H-MFI leads to a shorter distance between $H_3O^+_{hydr.}$, inducing a decrease in $d_{h\text{-}h}$, $d_{b\text{-}b}$, and $V_{b\text{-}b}$. Figure 3B shows that increasing the BAS concentration from 0.05 to 0.86 mmol/g_{MFI} reduced the $d_{h\text{-}h}$ from 2.6 to 1.0 nm and the $d_{b\text{-}b}$ from 1.6 to almost 0.0 nm. It should be noted here that the composition of $H_3O^+_{hydr.}$ [$H^+(H_2O)_8$] was determined to be invariant with temperature (supplementary text S3).

The individual energy levels of reaction ground and transition states in terms of enthalpy (ΔH°_{GS}, ΔH°_{TS}) and excess chemical potential (μ^{excess}_{GS}, μ^{excess}_{TS}) on all studied H-MFI are depicted as a function of $d_{b\text{-}b}$ (Fig. 3, C and D). The enthalpy of ground state ΔH°_{GS} of sorbed cyclohexanol is stable at a distance $d_{b\text{-}b}$ larger than 0.8 nm, whereas it increases sharply with the decrease of $d_{b\text{-}b}$, suggesting a repulsion between $H_3O^+_{hydr.}$ and sorbed cyclohexanol. The same trend is observed for μ^{excess}_{GS}. By contrast, the transition state has both ΔH°_{TS} and μ^{excess}_{TS} in reverse-volcano curves with the minimum at ~0.8 and ~0.6 nm of $d_{b\text{-}b}$. The $d_{b\text{-}b}$ of 0.8 nm is a critical distance at which $V_{b\text{-}b}$ is 0.2 nm^3, the same volume of one cyclohexanol molecule in liquid phase. At this distance, the volume between two neighboring $H_3O^+_{hydr.}$ is equal to the van der Waal (vdW) volume of cyclohexanol. At lower $d_{b\text{-}b}$, the $V_{b\text{-}b}$ becomes smaller than the vdW volume of cyclohexanol, causing a strong vdW repulsion that increases the energy of the transition state and decreases the TOF. In an open aqueous solution, the work to separate charges (hydronium ions and the anions of the zeolite) will be replaced only by a volume increase without constraining the sorbed alcohol.

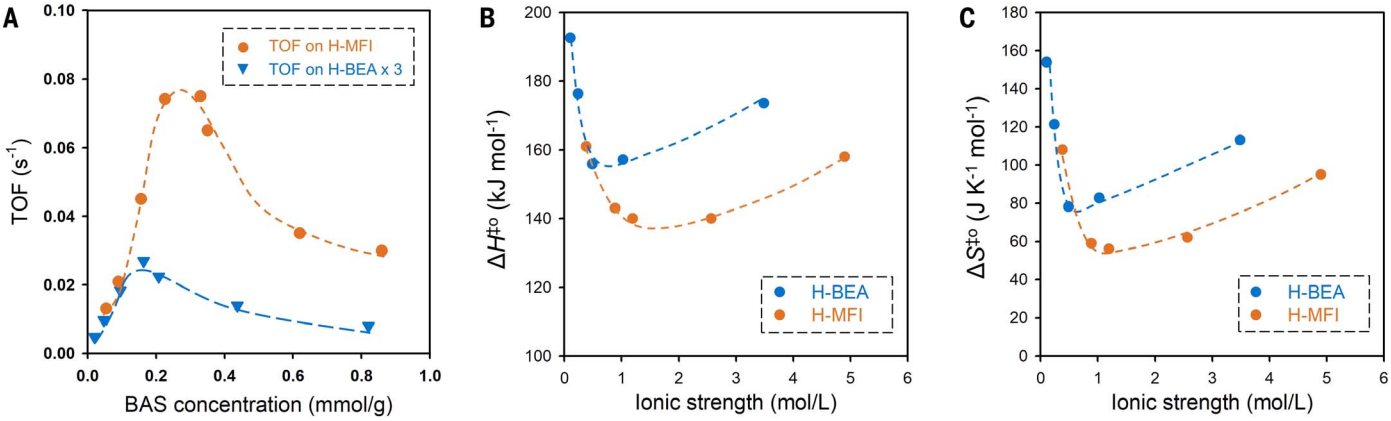

Fig. 4. Comparison of the dehydration reactions of cyclohexanol catalyzed by $H_3O^+_{hydr.}$ in H-MFI and H-BEA. (**A**) Impact of BAS concentration on the TOF at 423 K. (**B** and **C**) Activation enthalpy ($\Delta H^{\ddagger o}$) (B) and activation entropy ($\Delta S^{\ddagger o}$) (C) as a function of ionic strength.

Thus, we show how the bulkiness and the charges of $H_3O^+_{hydr.}$ constrained in zeolite micropores combine to influence the catalytic activity. For H-MFI, the $H_3O^+_{hydr.}$ is a cluster with a composition of $H^+(H_2O)_8$ and a specific volume, for example, ~0.24 nm^3 at room temperature. It is anchored to the exchange sites of the zeolite framework by Coulombic forces and competes with substrate (e.g., cyclohexanol) to occupy the micropore volume. Because the stabilization of water in the $H^+(H_2O)_8$ ion is larger than the stabilization of the sorbed organic molecule, that is, cyclohexanol, the latter adsorbs only in the volume between neighboring $H^+(H_2O)_8$ in the micropore channel. This adds spatial constraints to the substrate additional to that of the micropore framework. At high $H_3O^+_{hydr.}$ concentrations, the volume between neighboring $H^+(H_2O)_8$ becomes smaller than the vdW volume of substrate. This leads to strong vdW repulsion between substrate and $H^+(H_2O)_8$ and consequently results in a decrease in the reaction rate. Such vdW repulsion might not apply for the case of smaller alcohols, for example, ethanol, because they were shown to be capable of replacing water molecules in the $H_3O^+_{hydr.}$ cluster, forming $(C_2H_5OH)(H_3O^+)(H_2O)_n$ cluster in zeolite channels (*22*).

Thus, the charge of $H_3O^+_{hydr.}$ creates an ionic environment that can be expressed as the ionic strength in H-MFI micropores. Such an environment increases the standard free energy and excess chemical potential of the substrate ground state, that is, it destabilizes the uncharged reacting ground state of cyclohexanol. The ionic environment stabilizes the positively charged transition state. Both effects together lead to a decrease of the activation free energy and enhance the reaction rate. Such ionic environments in zeolites will also exist with other solvents. For example, methanol forms protonated clusters $H^+(CH_3OH)_n$ in small-pore zeolites (*23*), which would additionally allow for the stabilization of the charged transition state via the modulating solvent permittivity (*24*).

The combination of the enhancement by the charged environment and the limitations by the additional spatial constraints from $H_3O^+_{hydr.}$ leads to a maximum in the catalytic activity of $H_3O^+_{hydr.}$ with varying $H_3O^+_{hydr.}$ concentrations. For H-MFI, the highest rates are observed when the volume between two neighboring $H_3O^+_{hydr.}$ equals to the vdW volume of substrate, that is, the concentrations of substrate and $H_3O^+_{hydr.}$ in the micropores are almost equal.

The final question is, however, how general these conclusions about reactivity in constrained environments are. To probe this, we explored a wide series of H-BEA zeolites (table S1) and report here the first results of this study. The dependence of the rate of alcohol dehydration on the concentration of hydronium ions exhibits an analogous volcano-like dependence (Fig. 4A). In particular, the variation of activation enthalpy and entropy with ionic strength shows similar profile shapes to that of H-MFI (Fig. 4, B and C), indicating that the ionic strength influences catalytic activity through the same mechanism. Note the curves shifting up and toward lower ionic strength on H-BEA compared with H-MFI, which are attributed to the larger pore size of H-BEA that induces less vdW stabilization of transition state. It is to be expected that the specific enhancement and the position of the maximum will subtly depend on the size of the reacting molecule and the difference in polarity between the reacting substrate and the transition state. Overall, the results demonstrate unequivocally that the quantitative interpretation of the catalytic activity will allow for the prediction of the most suitable microporous catalyst for reactions in the presence of active sites that are associated with ions.

REFERENCES AND NOTES

1. R. Gounder, E. Iglesia, *J. Am. Chem. Soc.* **131**, 1958–1971 (2009).
2. P. Tian, Y. Wei, M. Ye, Z. Liu, *ACS Catal.* **5**, 1922–1938 (2015).
3. W. Vermeiren, J. P. Gilson, *Top. Catal.* **52**, 1131–1161 (2009).
4. E. T. C. Vogt, B. M. Weckhuysen, *Chem. Soc. Rev.* **44**, 7342–7370 (2015).
5. G. L. Woolery, G. H. Kuehl, H. C. Timken, A. W. Chester, J. C. Vartuli, *Zeolites* **19**, 288–296 (1997).
6. D. Barthomeuf, *J. Phys. Chem.* **88**, 42–45 (1984).
7. C. Mirodatos, D. Barthomeuf, *J. Catal.* **114**, 121–135 (1988).
8. H. Stach *et al.*, *J. Phys. Chem.* **96**, 8480–8485 (1992).
9. A. Auroux, *Top. Catal.* **4**, 71–89 (1997).
10. H. Shi, S. Eckstein, A. Vjunov, D. M. Camaioni, J. A. Lercher, *Nat. Commun.* **8**, 15442 (2017).
11. Y. Liu *et al.*, *Nat. Commun.* **8**, 14113 (2017).
12. S. Wang, E. Iglesia, *J. Catal.* **352**, 415–435 (2017).
13. A. J. Jones, S. I. Zones, E. Iglesia, *J. Phys. Chem. C* **118**, 17787–17800 (2014).
14. V. J. Margarit *et al.*, *ACS Catal.* **9**, 5935–5946 (2019).
15. S. Eckstein *et al.*, *Angew. Chem. Int. Ed.* **58**, 3450–3455 (2019).
16. S. Schallmoser *et al.*, *J. Catal.* **316**, 93–102 (2014).
17. W. O. Haag, R. M. Lago, P. B. Weisz, *Nature* **309**, 589–591 (1984).
18. D. J. Parrillo, C. Lee, R. J. Gorte, *Appl. Catal. A* **110**, 67–74 (1994).
19. A. Janda, A. T. Bell, *J. Am. Chem. Soc.* **135**, 19193–19207 (2013).
20. B. C. Knott *et al.*, *ACS Catal.* **8**, 770–784 (2018).
21. D. H. Olson, G. T. Kokotailo, S. L. Lawton, W. M. Meier, *J. Phys. Chem.* **85**, 2238–2243 (1981).
22. J. S. Bates, B. C. Bukowski, J. Greeley, R. Gounder, *Chem. Sci.* **11**, 7102–7122 (2020).
23. J. R. Di Iorio *et al.*, *J. Catal.* **380**, 161–177 (2019).
24. D. Y. Murzin, *Catal. Sci. Technol.* **6**, 5700–5713 (2016).
25. W. Luo *et al.*, *Green Chem.* **21**, 3744–3768 (2019).
26. Y. Zhi *et al.*, *J. Am. Chem. Soc.* **137**, 15781–15794 (2015).

ACKNOWLEDGMENTS

We thank O. Y. Gutiérrez and D. M. Camaioni for fruitful discussions and S. Prodinger and M. A. Derewinski for providing the H-BEA zeolite. **Funding:** This work (J.A.L. and S.K.) was supported by the U.S. Department of Energy (DOE), Office of Science, Office of Basic Energy Sciences (BES), Division of Chemical Sciences, Geosciences and Biosciences (Transdisciplinary Approaches to Realize Novel Catalytic Pathways to Energy Carriers, FWP 47319). N.P. and G.L.H. were supported by the DOE Office of Science and BES, Division of Chemical Sciences, Geosciences and Biosciences, under grant no. DE-FG02-01ER15183, to Yale University, Department of Chemical and Environmental Engineering. **Author contributions:** Yue L. and J.A.L. conceived the research; N.P. performed the

catalytic reaction by HCl and determined the activation energy on H-MFI; P.H.H., H.S., L.M., Yua.L., and E.B. measured the physicochemical property and catalytic activity of H-MFI, wherein P.H.H. first reported the volcano-like activity of H-MFI; S.E. and Q.L. measured the adsorption property of H-MFI; S.K. measured the reactions on H-BEA; and G.L.H. helped with data analysis.
Competing interests: The authors declare no competing interests.

Data and materials availability: All data are available within the main text and the supplementary materials.

SUPPLEMENTARY MATERIALS

science.sciencemag.org/content/372/6545/952/suppl/DC1
Materials and Methods
Supplementary Text S1 to S3
Figs. S1 to S5
Table S1
References (*27*–*29*)

2 March 2021; accepted 23 April 2021
Published online 6 May 2021
10.1126/science.abh3418